Available online at www.sciencedirect.com
ScienceDirect
Geochimica et Cosmochimica Acta 70 (2006) 4813–4825
Geochimica
www.elsevier.com/locate/gca

Diffusion induced Li isotopic fractionation during the cooling of magmatic rocks: The case of pyroxene phenocrysts from nakhlite meteorites

P. Beck [a,*], M. Chaussidon [b], J.A. Barrat [c], Ph. Gillet [a], M. Bohn [d]

[a] *Laboratoire des Sciences de la Terre, CNRS UMR 5570, Ecole Normale Supérieure de Lyon, 46 allée d'Italie, 69364 Lyon Cedex 7, France*
[b] *CRPG-CNRS UPR 2300, 15 rue Notre-Dame des Pauvres, 54501 Vandœuvre-les-Nancy Cedex, France*
[c] *CNRS UMR 6538 (Domaines Océaniques), U.B.O.-I.U.E.M., Place Nicolas Copernic, F-29280 Plouzané Cedex, France*
[d] *Ifremer-Centre de Brest, (CNRS-UMR 6538), BP70, 29280 Plouzané Cedex, France*

Received 13 September 2005; accepted in revised form 13 July 2006

Abstract

Ion-microprobe was used to measure Li abundances and isotopic compositions in pyroxenes from three Martian meteorites belonging to the nakhlite family. The profiles performed across augite crystals from Northwest Africa 817 show a large isotopic zoning from crystal cores (δ^7Li $\sim$ 0‰) to rims (δ^7Li $\sim$ +20‰) while Li abundances are almost constant ($\sim$9.2 μg/g). Unlike NWA 817, the pyroxene studied in the Miller Range 03346 nakhlite shows a zoning in Li abundance, with concentrations increasing from $\sim$2.5 μg/g in the core to $\sim$9 μg/g in the rim. The augite rim (δ^7Li = +7‰) is slightly enriched in ^{7}Li with regard to the core (δ^7Li = +4‰), but most of the isotopic variations observed occur at an intermediate position along the profile, where δ^7Li falls down to $\sim$−11‰. In the case of Nakhla, Li concentrations in augite increase from cores ($\sim$3.5 μg/g) to rims ($\sim$6.5 μg/g), while the δ^7Li variation is restricted (i.e., between δ^7Li = +6.0 and +12.6‰). For the three meteorites the Li abundances were also measured in the groundmass, which was found to be enriched in lithium ($\sim$10 μg/g). Conventional magmatic and post-magmatic processes such as alteration and fractional crystallization, fail to explain the dataset obtained on nakhlites. Degassing processes, which were previously proposed to explain the Li distribution in shergottite crystals, cannot result in the strong decoupling between Li abundances and isotopic composition observed in nakhlites. We suggest that the original magmatic Li distributions (concentrations and isotopic compositions) in nakhlites have been modified by diffusion of Li from the Li-rich groundmass towards the pyroxene crystals during sub-solidus cooling. Diffusion appears to have been efficient for NWA 817 and MIL 03346 but, apparently, did not produce a significant migration of Li in Nakhla, possibly because of the lower abundance of groundmass in the latter. Diffusion induced Li redistributions may also affect terrestrial porphyric rocks but very specific cooling rates are required to quench the diffusion profiles as observed in two of the present nakhlites.

1. Introduction

Lithium, the lightest lithophile element, possesses two stable isotopes, ^{6}Li (≈7.5%) and ^{7}Li (≈ 92.5%). The large range of variations of Li isotopic compositions observed in natural systems (≈60‰ range in ^{7}Li/^{6}Li ratios) has generated, during the last two decades, a growing interest in its geochemistry (e.g., Elliott et al., 2004; Tomascak, 2004 and references therein). Interestingly, this element is mobile when aqueous fluids are involved (Brenan et al., 1998b) and is now considered as a valuable proxy of metamorphic, hydrothermal and magmatic processes (Chan et al., 1993; You et al., 1995; Zack et al., 2003 and references therein). Lithium can thus be anticipated to be a powerful tracer for the petrogenesis of Martian rocks and to bring new

* Corresponding author. Present address: Geophysical Laboratory, Carnegie Institution of Washington, 5251 Broad Branch Road NW, Washington DC 20015-1305, USA.
E-mail addresses: pbeck@ciw.edu, pbeck@gl.ciw.edu (P. Beck).

0016-7037/$ - see front matter © 2006 Elsevier Inc. All rights reserved.
doi:10.1016/j.gca.2006.07.025

information on (i) possible fluid–rock interactions during the emplacement of Martian lavas or (ii) possible magmatic degassing of Martian melts.

Experimental petrology studies on Martian basaltic rocks, the so-called basaltic shergottites, imply that their parental magmas contained appreciable amounts of water (about 1.8 wt%) which was lost by degassing (Dann et al., 2001). Such a process may have left specific signatures in the Li distributions and isotopic compositions of phenocrysts from shergottites: in fact though Li is incompatible in dry basaltic melts, its concentration decreases from cores to rims in pyroxenes from the two shergottites Zagami and Shergotty (Lentz et al., 2001). Because Li is soluble in aqueous fluids (Brenan et al., 1998a), such pyroxene zonings may be explained by a coupled loss of H_2O and Li from the crystallizing magma (Lentz et al., 2001; Herd et al., 2004, 2005). This hypothesis was further tested by the study of the Li concentrations and isotopic compositions, which may be fractionated during degassing, in pyroxenes from the Northwest Africa 480 (NWA 480) shergottite (Beck et al., 2004). A large increase from a ^{7}Li depleted core ($\delta^7Li = -17‰$) towards a ^{7}Li enriched rim ($\delta^7Li = +10‰$) was observed in NWA 480.

However, Li is one of the fastest elements for solid state diffusion (Giletti and Shanahan, 1997) and two different lines of evidence strongly suggest that the pristine Li distribution inherited from magmatic processes can be strongly perturbed because of the strong mobility of Li (and its isotopes) in mineral phases. First, the pyroxenes from the Pasamonte eucrite, which formed from an anhydrous melt, exhibits evidences of re-mobilization of Li during or subsequent to its crystallization, shock induced Li diffusion being an additional process which could obscure the magmatic Li distribution (Herd et al., 2004). Second, it has been recently shown that olivine and pyroxene phenocrysts in the NWA 479 lunar basalt, also crystallized from a dry melt, display a wide range of δ^7Li values (from 0‰ to +16‰) which has been ascribed to a post-magmatic diffusion of Li from the groundmass into the crystals (Barrat et al., 2005).

There is thus an obvious need for a better understanding of the behavior of Li (and its isotopes) during late- and post-magmatic evolution. During a reconnaissance study of Li isotopes in Martian meteorites, we found that the pyroxenes of the Northwest Africa 817 nakhlite (NWA 817) display a prominent zoning, from $\delta^7Li = +1‰$ in the cores to +21‰ in the rims. This observation encouraged us to undertake a detailed study of the Li systematics in phenocrysts of nakhlites, which because of their size, shapes and high Li concentrations are particularly well suited for an ion microprobe study of Li. In addition to NWA 817, we selected Nakhla and Miller Range 03346 (MIL 03346). The different Li and ^{7}Li/^{6}Li systematics observed in these three nakhlites evidence the prominence of post-magmatic perturbations for Li in Martian rocks. These perturbations can be explained in a model where the Li concentration gradients inherited from the magmatic history are progressively relaxed by solid state diffusion in the crystals during the cooling of the rock. Such a diffusion process produces characteristic Li isotopic variations in pyroxenes.

2. Ion and electron microprobe analysis

The Li concentrations and isotopic compositions were obtained by ion microprobe analysis with the ims 3f instrument at CRPG-CNRS (Nancy) using classical procedures (Chaussidon and Robert, 1998; Beck et al., 2004; Barrat et al., 2005, and references therein). The Li concentrations and isotopic compositions were determined at a mass resolution ($M/\Delta M$) of 1200 (to remove the interfering $^6LiH^+$ at mass 7) by classical energy filtering (-60 ± 10 V) for concentrations and with the energy slit centered and fully opened for isotopic ratios. The samples were sputtered by a O^- primary beam (≈50 nA) of ≈25 μm wide. Secondary ions were accelerated at 4.5 kV. Positive ions of ^{6}Li and ^{7}Li were detected by magnetic peak switching on the electron multiplier (background and dead time of 0.05 count/s and 44 ns, respectively). The set of silicate glass and mineral standard used (Decitre et al., 2002; Beck et al., 2004; Table 1) allowed to determine the ion yield of Li relative to Si (yield Li $= (Li^+/Si^+)/(Li/Si)$) and the instrumental mass fractionation of Li isotopes ($\alpha_{inst}Li = (^7Li/^6Li)_{measured}/(^7Li/^6Li)_{true}$).

The yield Li-value determined for one of our silicate glass (with 63.4 μg/g Li) was of 1.44 ± 0.02 (6 analyses). It was reproducible to within ±4% relative on one of our clinopyroxene standard (cpx BZ 226) having a much lower Li content (5.9 μg/g Li). No significant matrix effects, at these low Li concentrations, have ever been observed with our set of standards (Decitre et al., 2002; Beck et al., 2004; Barrat et al., 2005). The Li concentrations are thus given in Tables 2 and 3 with an error of ±5% relative (one sigma).

The isotopic ratios are given in Tables 2 and 3 in δ-units using the δ^7Li notation ($\delta^7Li = 1000 \times [(^7Li/^6Li)_{sample}/$

Table 1
Chemical composition of the standard materials used for Li abundance and Li isotopes measurements (opx, orthopyroxene; cpx, clinopyroxene)

	Nazca (glass)	BZ226 (opx)	BZ226 (cpx)	BZCG (cpx)
Oxyde wt%				
SiO_2	48.69	54.14	51.36	50.35
Al_2O_3	14.07	3.85	4.49	7.05
MgO	8.41	31.20	15.35	14.11
FeO	10.74	9.11	3.63	2.96
TiO_2	1.80	0.06	0.26	0.37
Na_2O	2.63	0.04	0.81	1.32
K_2O	0.066	0.014	0.005	0.008
CaO	10.74	0.46	22.23	21.71
Mg#	58.3	85.9	88.3	89.5
Mg/Si	0.26	0.86	0.44	0.42
Li (ppm)	5	3.7	5.9	—
δ^7Li (‰)	+5.8 ± 1.1	−4.2 ± 1.0	−4.1 ± 1.0	+10.5 ± 1.0

Table 2
Li abundances and isotopic compositions measured in augite and olivine from Nakhla and NWA 817

	Distance to core (μm)	Distance to rim (μm)	Composition	Mg#	TiO_2 (wt%)	Na_2O (wt%)	Li (μg/g)	δ^7Li (‰)
Nakhia								
Pyroxenes								
px1 #1	0	110	$En_{36.4}Wo_{38.0}Fs_{25.5}$	58.8	0.36	0.23	4.6	+9.6 ± 2.1
px1 #2	85	25	$En_{38.4}Wo_{38.0}Fs_{23.6}$	61.9	0.13	0.15	6.3	+6.8 ± 2.1
px1 #3	90	15	$En_{37.0}Wo_{37.9}Fs_{25.1}$	59.5	0.15	0.18	3.0	+9.8 ± 2.3
px1 #4	75	85	$En_{36.9}Wo_{39.8}Fs_{23.3}$	61.3	0.43	0.24	3.2	+7.4 ± 1.8
px2 #5	185	20	$En_{34.1}Wo_{37.9}Fs_{28.0}$	54.9	0.19	0.16	6.8	+6.0 ± 1.7
px2 #6	10	140	$En_{33.9}Wo_{37.4}Fs_{28.7}$	54.1	0.17	0.23	4.1	+12.6 ± 2.4
px3 #7	125	15	$En_{39.3}Wo_{37.7}Fs_{23.0}$	63.1	0.14	0.16	6.6	+6.4 ± 2.0
Olivines								
ol1 #9	0	170	$Fa_{68.4}$	31.6	0.02	0.00	2.3	+10.2 ± 2.4
ol2 #10	185	15	$Fa_{65.8}$	34.2	0.00	0.01	3.4	+13.3 ± 2.5
NWA 817								
Pyroxenes								
px1 #1	165	15	$En_{33.6}Wo_{40.3}Fs_{26.1}$	56.3	0.36	0.31	8.3	+16.8 ± 0.6
px1 #2	130	34	$En_{37.1}Wo_{40.3}Fs_{22.6}$	62.1	0.24	0.39	9.6	+12.2 ± 0.7
px1 #3	95	53	$En_{36.8}Wo_{40.8}Fs_{22.4}$	62.2	0.33	0.37	9.1	+7.4 ± 0.6
px1 #4	55	71	$En_{36.5}Wo_{40.1}Fs_{23.4}$	60.9	0.12	0.33	8.9	+3.5 ± 0.7
px1 #5	20	90	$En_{36.9}Wo_{40.4}Fs_{22.7}$	61.9	0.22	0.30	10.0	+1.0 ± 0.6
px1 #6	20	90	$En_{36.9}Wo_{40.3}Fs_{22.8}$	61.8	0.32	0.33	10.0	+3.9 ± 0.9
px1 #7	55	71	$En_{36.9}Wo_{39.9}Fs_{23.2}$	61.5	0.33	0.39	8.9	+8.1 ± 0.6
px1 #8	95	53	$En_{36.2}Wo_{39.8}Fs2_{4.0}$	60.1	0.23	0.35	9.9	+3.5 ± 0.6
px1 #9	130	34	$En_{37.3}Wo_{39.4}Fs_{23.3}$	61.5	0.29	0.29	9.1	+14.4 ± 0.8
px1 #10	165	15	$En_{36.4}Wo_{41.0}Fs_{22.6}$	61.7	0.25	0.29	9.0	+14.9 ± 0.6
px2 #18	190	15	$En_{15.9}Wo_{42.3}Fs_{41.8}$	27.6	1.14	0.46	10.0	+20.6 ± 1.0
px2 #19	150	34	$En_{37.1}Wo_{40.5}Fs_{22.4}$	62.4	0.25	0.31	8.8	+15.1 ± 1.1
px2 #20	105	53	$En_{37.3}Wo_{40.3}Fs_{22.4}$	62.5	0.27	0.34	9.0	+11.1 ± 1.2
px2 #21	65	71	$En_{37.0}Wo_{40.4}Fs_{22.6}$	62.0	0.29	0.34	9.3	+8.7 ± 2.8
px2 #22	20	90	$En_{36.8}Wo_{40.2}Fs_{23.0}$	61.5	0.32	0.34	9.4	+7.7 ± 1.4
px2 #23	20	90	$En_{36.7}Wo_{40.7}Fs_{22.6}$	61.9	0.30	0.34	8.9	+0.9 ± 1.3
px2 #24	65	71	$En_{37.9}Wo_{39.3}Fs_{22.8}$	62.4	0.28	0.36	9.1	+5.5 ± 1.4
px2 #25	105	53	$En_{37.4}Wo_{39.5}Fs_{23.1}$	61.8	0.26	0.32	9.0	+3.8 ± 1.3
px2 #26	150	34	$En_{36.7}Wo_{40.7}Fs_{22.6}$	61.9	0.28	0.32	9.2	+11.2 ± 1.4
px2 #27	190	15	$En_{36.7}Wo_{40.4}Fs_{22.9}$	61.6	0.26	0.31	9.1	+19.5 ± 1.4
Olivines								
ol1 #36	0	275	$Fa_{57.1}$	42.9	0.00	0.03	7.8	−1.9 ± 1.4
ol1 #38	350	15	$Fa_{76.1}$	23.9	0.04	0.02	13.9	+7.6 ± 1.2
ol2 #46	0	250	$Fa_{56.2}$	43.8	0.03	0.03	7.0	−0.1 ± 1.4
ol2 #51	400	15	$Fa_{58.1}$	41.9	0.00	0.02	5.3	+9.4 ± 1.6

Major element features of the analyzed areas are also given. Electron microprobe analyses were carried out at Ifremer (Centre de Brest) with a Cameca SX50. Analyses were generally obtained at 15 kV accelerating voltage with a sample current of 12 nA.

Table 3
Li abundances and isotopic compositions of a profile in an augite crystal from MIL 03346

	Distance to core (μm)	Distance to rim (μm)	Composition (mol%)	Mg#	TiO_2 (wt%)	Na_2O (wt%)	Li (μg/g)	δ^7Li (‰)
MIL 03346,6								
Pyroxene								
px1 #1	300	15	$En_{36.5}Wo_{40.8}Fs_{22.7}$	61.6	0.29	0.26	9.7	+4.7 ± 0.6
px1 #2	240	72	$En_{36.3}Wo_{40.8}Fs_{22.8}$	61.4	0.36	0.25	3.7	+2.8 ± 0.5
px1 #3	180	129	$En_{35.5}Wo_{40.8}Fs_{23.7}$	59.9	0.26	0.24	5.5	−5.1 ± 0.7
px1 #4	120	186	$En_{36.3}Wo_{40.5}Fs_{23.3}$	61.1	0.37	0.27	2.6	−11.3 ± 0.6
px1 #5	60	243	$En_{35.5}Wo_{41.4}Fs_{23.1}$	60.5	0.18	0.23	2.5	−2.1 ± 0.6
px1 #6	0	300	$En_{36.4}Wo_{41.3}Fs_{22.3}$	62.0	0.24	0.24	2.6	+2.3 ± 0.7
px1 #7	60	243	$En_{35.8}Wo_{41.2}Fs_{23.0}$	60.9	0.23	0.32	9.7	+4.2 ± 0.7
px1 #8	120	186	$En_{35.9}Wo_{41.2}Fs_{22.9}$	61.1	0.29	0.28	3.9	−1.6 ± 0.7
px1 #9	180	129	$En_{35.5}Wo_{41.6}Fs_{22.9}$	60.8	0.29	0.27	2.3	−6.3 ± 0.7
px1 #10	240	72	$En_{36.1}Wo_{40.7}Fs_{23.2}$	60.8	0.23	0.30	4.5	−11.8 ± 1.0
px1 #11	300	15	$En_{25.4}Wo_{38.6}Fs_{36.1}$	41.3	0.61	0.26	7.8	+8.0 ± 0.6

Major element features of the analyzed areas are also given. Electron microprobe analyses were carried out at Ifremer (Centre de Brest) with a Cameca SX50. Analyses were generally obtained at 15 kV accelerating voltage with a sample current of 12 nA.

($^7Li/^6Li)_{LSVEC}$-1]), LSVEC being the international carbonate standard for Li isotopes (Flesh et al., 1973).

The values of $\alpha_{inst}Li$ determined on our standards (Table 1) range from ≈1.021 to ≈1.032 during the different analytical sessions. The major reasons for this variation of $\alpha_{inst}Li$ over the different analytical sessions are (i) variations in the efficiency of the electron multiplier, isotopic fractionation on the first dynode increasing with ageing of the multiplier and (ii) differences in the secondary settings. We also observed variations of $\alpha_{inst}Li$ during a given session before and after cleaning of the duoplasmatron source: this is most probably due to small changes in the shape and/or density of the primary beam. All these changes were monitored by running our standards or by duplicating at the end of an isotopic profile the first point of the profile. Typical reproducibilities (given below at ±1 sigma) obtained for $\alpha_{inst}Li$ on our standards during an analytical sessions are ±1.0‰ ($n = 3$) for cpx BZ 226 and ±0.5‰ ($n = 5$) for cpx BZ 226. The precision of the Li isotopic measurements given in Tables 2 and 3 range from ±0.7‰ (1 sigma) to ±2.8‰ (1 sigma): they were determined from (i) the counting statistics, (ii) the error on correction for instrumental mass discrimination and (iii) the external reproducibility.

The presence of matrix effects on Li isotope measurements was tested by repeated analysis of different silicate mineral and glass standards of variable Li abundance and isotopic composition (Table 1). Possible effects for this range of chemical composition are inferior to 2‰ (Beck et al., 2004), thus well below the isotopic variations reported in the meteorites studied here. Furthermore, we can remark that most of the isotopic variations we will describe in nakhlites occur in crystal core, thus at constant major element composition. The absence of correlation between measured Li isotopic composition and major elements composition, (shown in Fig. 2 for the Fe/(Fe + Mg) ratio) is an other indication of the low intensity of matrix effects, within this range of chemical compositions.

Major and minor element abundances were measured using a CAMECA SX50 electron microprobe (IFREMER-Centre de Brest). Analyses were obtained using mineral and oxide standards at an accelerating voltage of 15 kV, a probe current of 12 nA and a one micron beam diameter. Compositions were determined in the same regions where ion probe measurements were performed.

3. Sample description

Nakhlites have been extensively studied during the last ten years. The reader is referred to the up-to-date review by Treiman (2005) for petrographic descriptions and major element compositions of their phases. The following polished sections were used in the present study: Nakhla (Muséum National d'Histoire Naturelle de Paris, n° 1226), Northwest Africa 817 (Ecole normale supérieure

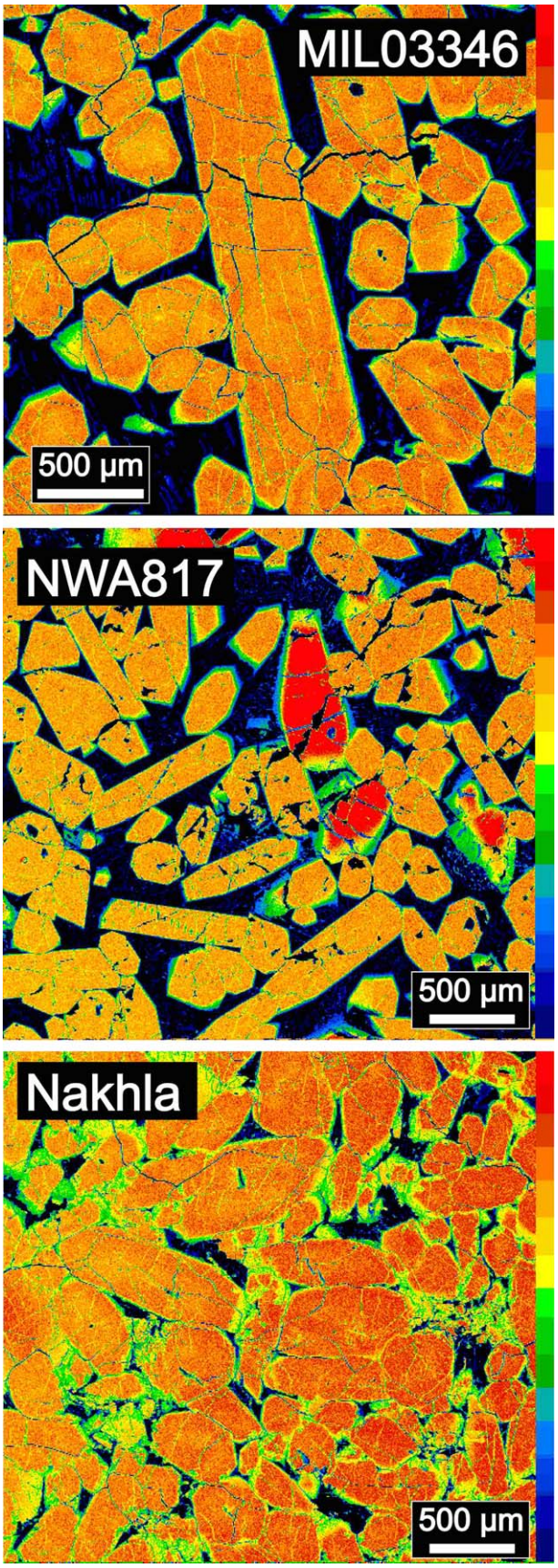

Fig. 1. Mg distribution maps of polished sections of MIL 03346, NWA 817, and Nakhla. Zoned augite crystals are mainly orange and groundmass is dark. Olivines (red) are seen here only in NWA 817.

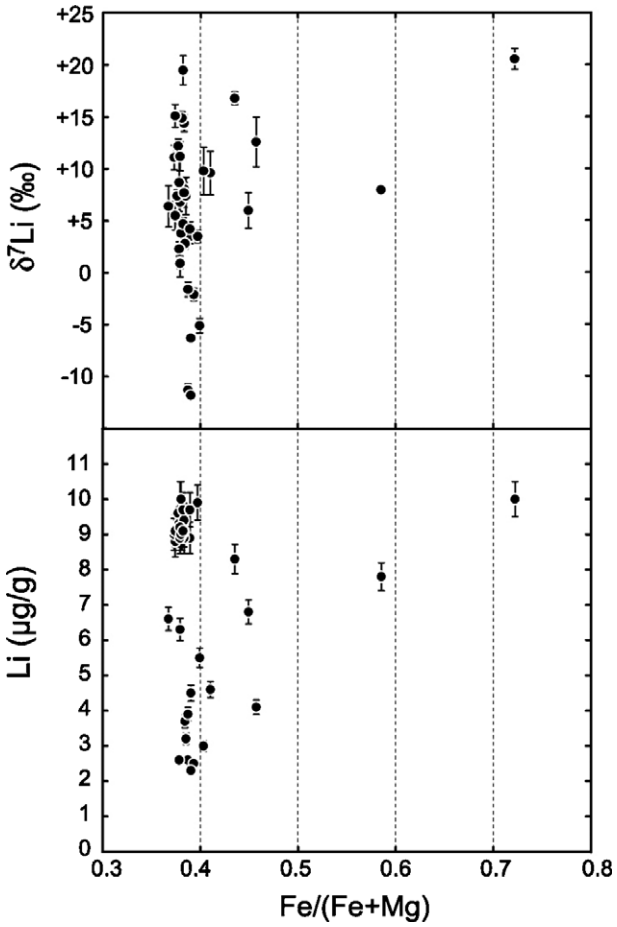

Fig. 2. Variation of δ^7Li and [Li] relative to atomic Fe/(Fe + Mg) in pyroxenes from the three studied nakhlites.

de Lyon, NWA 817-B), and Miller Range 03346 (section MIL 03346,6 provided by the Meteorite Working Group). The main features of these three nakhlites are briefly summarized below.

Nakhlites are igneous cumulate rocks composed mostly of subhedral to euhedral augite (69–81 vol %), olivine (0–13 vol %) set in a groundmass (8–23 vol %) made chiefly of radiating sprays of plagioclase laths with titanomagnetite for Nakhla, of Fe_2O_3-rich plagioclase laths, skeletal titanomagnetite crystals, needle shaped augite and olivine crystals in a very fine-grained matrix for NWA 817, or of glass containing skeletal crystals of olivine, titanomagnetite and pyrrhotite for MIL 03346. In the three studied nakhlites, the pyroxene crystals display a large homogeneous core, with Mg/(Mg + Fe) about 0.60–0.65, surrounded by distinct rim zones richer in Fe (Fig. 1). The transitions from core to rims are sharp in NWA 817 and MIL 03346, and are more gradual in Nakhla (Fig. 1). Rims are generally lacking where pyroxene crystals abut on other phenocrysts. Olivine is absent in the MIL 03346,6 section. In Nakhla and NWA 817, olivine grains display a normal zoning from Fa_{70} to Fa_{83}, and from Fa_{59} to Fa_{86}, respectively.

Finally, it is important to stress that nakhlites contain pre-terrestrial (i.e., Martian) veinlets or patches of alteration phases such as smectite clay, Fe-oxy-hydroxides, salt minerals (e.g., halite and gypsum), and sometimes carbonates deposited by water (e.g., Bridges and Grady, 2000; Gillet et al., 2002; Sautter et al., 2002; Treiman, 2005). In addition, NWA 817 and MIL 03346 are Saharan and Antarctic finds, respectively, so that they have been exposed to terrestrial weathering.

4. Results

About 40 points were analyzed for Li abundances and isotopic compositions in the three sections. These results, as well as the major element features of the analyzed areas are given in Tables 2 and 3. Li abundance and isotopic composition profiles obtained on pyroxene from the three nakhlites differ. Li abundances are constant in NWA 817, while they show an increase from cores to rims in Nakhla and MIL 03346. A large isotopic variation (>20‰) is present in NWA 817 and MIL 03346 while it is more restricted in Nakhla (~8‰). For the three samples, there is a strong decoupling between [Li] and δ^7Li.

4.1. Li concentration and isotopic composition in Nakhla

4.1.1. Augite

For the three grains analyzed, augite exhibits an increase of Li concentrations from 3.5 µg/g in the cores toward 6.5 µg/g in the rims (Fig. 3 and Table 2). These values are in agreement with both bulk rock measurements (Dreibus et al., 1982) and the values obtained on other sections of the same meteorite (Lentz et al., 2001). Li isotopic compositions show a restricted variation from δ^7Li = +6.0 to 12.6‰. These values are higher than the bulk rock measurement of Nakhla (δ^7Li = +4.5 ± 0.2‰) (Bridges et al., 2005).

4.1.2. Olivine

For both core and rim of the selected crystal, Li concentration approaches augite core values. The δ^7Li obtained is close to that of pyroxene within error (δ^7Li = +11.9 ± 1.6‰, $n = 3$).

4.1.3. Groundmass

Only one spot was performed for Li abundance determination ([Li] = 10.0 ± 0.5 µg/g).

4.2. Li concentration and isotopic composition in Northwest Africa 817

4.2.1. Augite

Two profiles were performed on two distant crystals. In both cases, Li abundances are constant, with a mean of 9.2 ± 0.2 µg/g ($n = 20$) (Fig. 4 and Table 1). These values are twice times higher than previous measurement in a pyroxene from the same meteorite (Musselwhite et al., 2005). The isotopic composition reveals a large increase

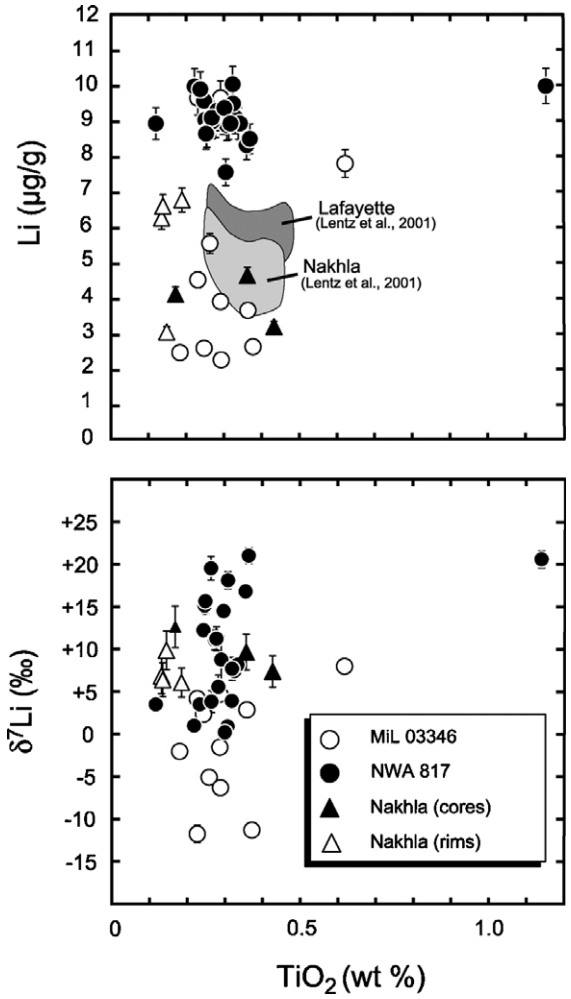

Fig. 3. Variations of Li and δ^7Li relative to TiO_2 in nakhlite augites.

from cores (δ^7Li ≈ 0‰) to rim (δ^7Li ≈ +20‰) for the two crystals (Fig. 4).

4.2.2. Olivine

Li concentrations are uniformly distributed in olivine ([Li] = 7.1 ± 0.75 µg/g, $n = 9$). As well as in pyroxene, a core/rim variation in isotopic composition is present. The extent is however smaller than in pyroxene. The measurements performed in crystal core from two distinct olivines gave δ^7Li = −1.9 ± 1.4‰ and −0.1 ± 1.4‰, while the values measured for the respective rims are δ^7Li = +7.6 ± 1.2‰ and δ^7Li = +9.4 ± 1.6‰.

4.2.3. Groundmass

Li concentrations in the groundmass are difficult to determine due to the large ion-probe beam size with regard to groundmass crystals size. Then, the measured value is dependant of the amount of plagioclase and pyroxene microliths in the analyzed area. Three measurements were performed, and illustrated this heterogeneity ([Li] = 4.5 ± 0.2, 19.6 ± 1.0, and 18.5 ± 0.9 µg/g).

4.3. Li concentration and isotopic composition in Miller Range 03346

4.3.1. Augite

One profile was realized across the width of the largest augite crystal (Figs. 1 and 5). Excepted for an anomalous point found in the section (Table 2, px1–7 having 9.7 µg/g lithium), the Li concentrations in the core are low (~2.5 µg/g) and increase to the rim (~9 µg/g). The isotopic composition measured along the profile is however unusual (Fig. 4). Augite rim (δ^7Li = +7‰) is slightly enriched in ^{7}Li with regard to its core (δ^7Li = +4‰), but most of the variation occur at intermediate position along the profile, where δ^7Li falls down to ≈−11‰.

4.3.2. Groundmass

A single spot was done for Li abundance determination ([Li] = 8.7 ± 0.3 µg/g).

4.4. Li balance and comparison with bulk rock measurements

4.4.1. Li abundance

Bulk rock values can be estimated using olivine, pyroxene and groundmass Li concentration, combined with mineral mode for each meteorites and phases densities. These calculations result in Li abundances of 5.1, 6.3, and 9.5 µg/g for Nakhla, MIL 03346, and NWA 817, respectively. In the case of Nakhla, this estimate compares well with bulk rock measurements ([Li] = 4.8 µg/g, Magna et al., 2006; [Li] = 6.3 µg/g, Seitz et al., 2006). The value obtained for MIL 03346 (6.3 µg/g) and NWA 817 (9.5 µg/g) are slightly higher than bulk rock estimate (MIL 03346, [Li] = 4.25 µg/g, Barrat et al., 2006; NWA 817, [Li] = 7.43 µg/g, Sautter et al., 2002) but these differences can be attributed to heterogeneity among samples of a same meteorite, particularly variability in groundmass abundance.

4.4.2. Li isotopic composition

The lack of Li isotopic composition measurement in the groundmass prohibits a reliable estimate of the bulk rock abundance from individual phase measurements. We can however at first order compare bulk augite Li isotopic composition (spherical weighted average) with bulk rock measurements available for Martian meteorites. Among the Martian meteorites suite, δ^7Li ranges between −0.6 ± 0.5 and +5.2 ± 0.5‰ (Seitz et al., 2006; Magna et al., 2006). Bulk augite estimates agrees for Nakhla (δ^7Li = +8.0‰) and MIL 03346 (δ^7Li = +2.9‰) with this values taking into account the total error on ion-probe measurements. In the case of NWA 817, bulk augite isotopic composition (δ^7Li = +12.0‰) is heavier than available data for Martian meteorites. The reason for this difference is not understood yet. In the case of the moon, where a large range of δ^7Li values from 0‰ to +16‰ (Barrat et al., 2005) has been found at the micrometer scale, one sam-

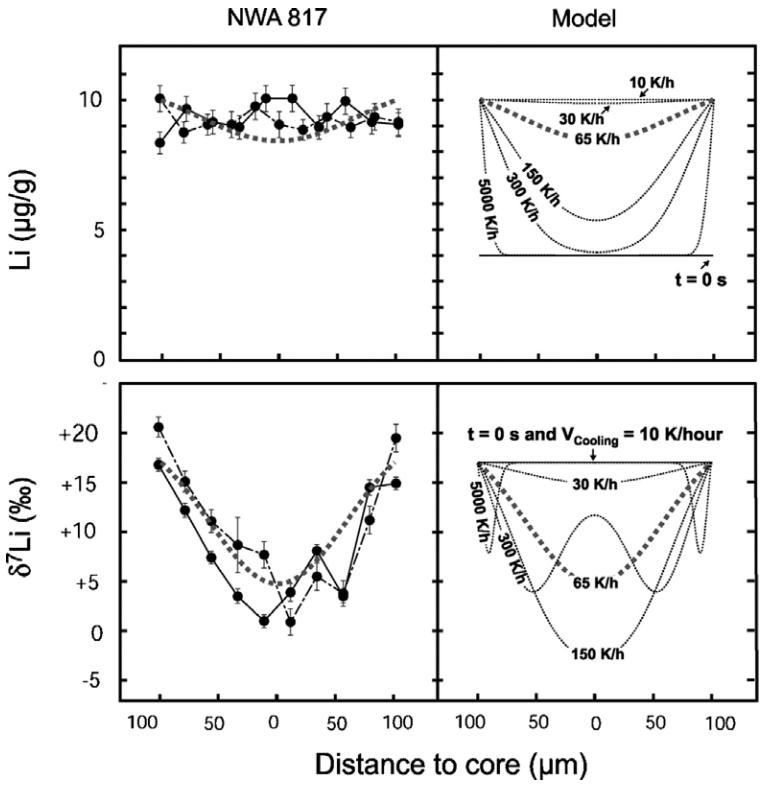

Fig. 4. Li abundance and isotopic composition distribution across two augite crystals in NWA 817. The observed and calculated diffusion profiles are compared (see the text for more details).

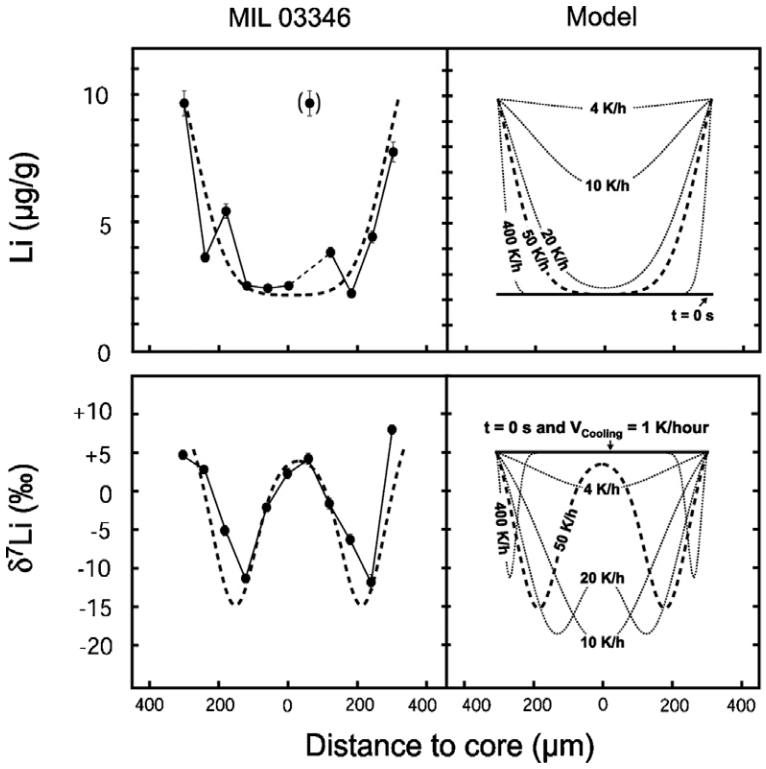

Fig. 5. Li abundance and isotopic composition distribution across a large augite crystal in MIL 03346. The observed and calculated diffusion profiles are compared (see the text for more details).

ple was recently found to have in bulk a very high δ^7Li value ($+18.4 \pm 1.2$, Seitz et al., 2006). This is not the case for Mars yet.

5. Discussion

5.1. A non "classical" origin for the δ^7Li variations in pyroxenes from nakhlites

The Li distribution observed in the pyroxenes from the three nakhlites, especially from NWA 817 and MIL 03346, cannot result from the processes classically invoked to explain isotopic variations in magmatic rocks, namely (i) source effects, (ii) assimilation–fractionation–crystallization (AFC model, DePaolo, 1981), (iii) degassing, and (iv) post-magmatic alteration. In fact, none of the above processes is able to produce the major characteristic of the present Li distributions: a clear zoning of the pyroxenes in either δ^7Li or [Li] (or both) with no simple correlation either between the δ^7Li and/or [Li] and the major or trace element concentrations (Tables 2, 3 and Fig. 3) or between the δ^7Li and the 1/[Li] (Fig. 6).

The low [Li] observed in the core of pyroxene from MIL 03346 (Fig. 5) seems at first glance broadly consistent with a magmatic fractionation because Li is moderately incompatible during the crystallization of olivine, pyroxene and plagioclase (Brenan et al., 1998a; Herd et al., 2004, 2005; Zanetti et al., 2004). However the large range of variations of δ^7Li values in this pyroxene, as well as in the one from NWA 817, cannot result from a closed system magmatic evolution for two reasons. First, Li is amongst the elements with the fastest diffusivity in melts (e.g., $D = 6 \times 10^{-5}$ m^2/s at 1400 °C, Richter et al., 2003) so that any Li isotopic heterogeneity of the mantle source of nakhlite would be erased during the melting episode. Second, fractional crystallization is unable to fractionate Li isotopes by more than ≈1‰ (Tomascak et al., 1999).

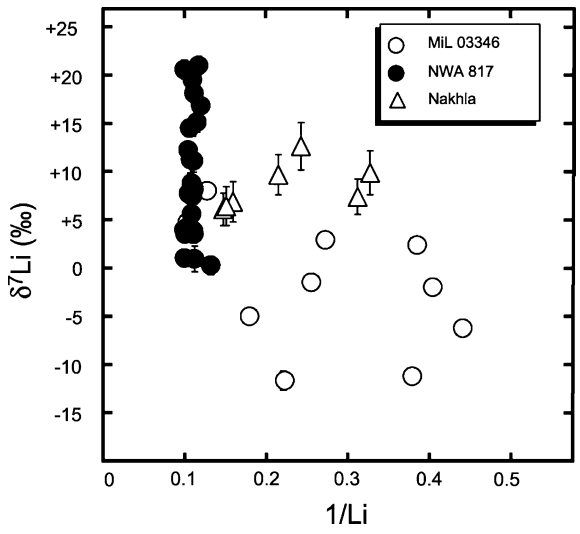

Fig. 6. Variation of δ^7Li relative to 1/[Li] in nakhlites.

AFC or degassing processes seem also unable to reproduce the diversity of the [Li] and δ^7Li profiles observed in the present pyroxenes. This comes from the fact that all the models which imply an open system for Li should a priori result in some kind of mixing relationship between [Li] and δ^7Li, which is not observed (Fig. 6). To produce δ^7Li variations in the melt and in the growing crystals with no correlation with the [Li] of the crystal, or with a constant [Li] such as in NWA 817, would require a perfect Li mass balance between the gain due to fractionation and the loss due for instance to degassing. Though such models cannot be totally excluded, they appear rather adhoc.

Thus, it seems obvious that the Li distributions observed in the pyroxenes are not inherited directly from the magmatic history but, most likely, have been strongly perturbed. There is no argument to support that this post-magmatic perturbation is related to the Martian and/or terrestrial low temperature alterations which have been evidenced from the presence of low temperature minerals (see Section 3). In fact, any significant low temperature addition to these rocks of Li having a different δ^7Li value would result in correlations (i.e., mixing lines) between 1/[Li] and the δ^7Li values. In addition, the profiles performed in large pyroxene crystals in NWA 817 and MIL 03346 do not present any anomalous [Li] or δ^7Li value near cracks, which are inferred to be zones of preferential circulation of secondary fluids. Therefore, it appears that the Li distribution observed in the pyroxenes from nakhlites imply the existence of an unusual process able to mobilize Li and to fractionate its isotopes in a rock in closed system at a post-magmatic stage.

5.2. Diffusion-induced kinetic isotopic fractionation of Li: the limits of the model

Theoretical considerations (Jambon, 1980; Richter et al., 1999, 2003) suggest that, because of their large relative mass difference, ^{7}Li and ^{6}Li should diffuse at significantly different rates in presence of a Li concentration gradient. Very few examples of such a process have yet been found in terrestrial rocks (Lundstrom et al., 2005; Teng et al., 2006). Recently, δ^7Li variations observed in olivine and pyroxene crystals from lunar basalt NWA 479 have been tentatively ascribed to diffusion induced Li isotopic fractionation (Barrat et al., 2005). It is a matter of fact that, in magmatic systems, Li concentrations are heterogeneously distributed during the crystallization of the minerals. Crystals display significantly lower Li abundances than surrounding melts ($D_{Li} \sim 0.2$–0.3 for olivine and pyroxene, Herd et al., 2004; Zanetti et al., 2004 and references therein) so that at the end of the magmatic evolution early phenocrysts can be embedded in a groundmass with significantly higher [Li]. Upon cooling and crystallization of the intercumulus liquid, Li can be expected to partition preferentially in pyroxene rather than mineral phases encountered in the groundmass. The behavior of Li during the crystallization of basalt supports this hypothesis.

Experimental petrology suggests that during the crystallization of basaltic melt, Li is preferentially incorporated in melt rather than in pyroxene in equilibrium with it (Brenan et al., 1998a; Herd et al., 2002). However, below the solidus, Li partitions preferentially in pyroxene rather than lately crystallized feldspar (Coogan et al., 2005).

We model in the following the Li behavior which can be anticipated from diffusion processes taking place in such a rock upon its cooling.

Models were computed using an explicit finite difference method (Crank, 1967) to solve the diffusion equation for an infinite cylinder geometry, which approximates the augite prisms:

$$\frac{dC}{dt} = D\left(\frac{d^2C}{dr^2} + \frac{1}{r}\frac{dC}{dr}\right) \quad (1)$$

C is the concentration, t is the time, and r is the distance to the revolution axis. D is the diffusion coefficient which is temperature dependent. This equation is solved simultaneously for ^{6}Li and ^{7}Li, which enables to calculate the evolution of both concentration ($[Li] = [^6Li] + [^7Li]$) and δ^7Li. The model assumes that (i) the rim of the crystal is in contact with a reservoir of constant concentration and isotopic composition which corresponds to the groundmass (ii) the partitioning coefficient of Li between the two solid phases is equal to 1, (iii) ^{7}Li and ^{6}Li fluxes are null at the crystal core because of crystal symmetry and (iv) the crystals were homogeneous before diffusion and shared the same Li isotopic composition than the residual melt (now the groundmass), i.e., that Li isotopic equilibrium was present at magmatic temperatures (Tomascak et al., 1999). Calculations were run at varying temperatures, using a linear cooling rate from a starting temperature T_0.

Solving Eq. (1) requires to know, or to postulate, values for (i) the ratio between the diffusion coefficients of ^{7}Li and ^{6}Li, (ii) the diffusion coefficient of Li in pyroxene, (iii) the cooling rate and the initial temperature, and (iv) the Li concentration ratio between the groundmass and the crystal.

The diffusion parameters for Li in pyroxene were taken according to Coogan et al. (2005). The ratio between the diffusion coefficients of ^{7}Li and ^{6}Li is expressed as $D_7/D_6 = (m_6/m_7)^\beta$, where D_6 and D_7 are the diffusion coefficients for ^{6}Li and ^{7}Li, respectively, and m_6 and m_7 are the atomic masses of ^{6}Li and ^{7}Li, respectively. The β parameter which ranges between 0 and 0.5 defines the strength of the so-called "isotope effect". A low value for β implies similar diffusivities for the two isotopes while a high-value imply a strong isotope effect, in other terms that the lighter isotopes will diffuse significantly faster than the heavier ones. β is controlled directly by the mechanisms of diffusion, more precisely by the correlation of consecutive jumps of the diffusing atom in the crystal lattice. The ratio of the diffusion coefficient for two isotopes can then be used to investigate diffusion mechanisms in solids (Peterson and Chen, 1974). In the case of Li, little is known on its diffusion mechanism in pyroxene and the β parameter has not been determined. However, Li diffusion coefficients measured in albite and pyroxene (Giletti and Shanahan, 1997; Coogan et al., 2005) are typically 3–5 orders of magnitude higher that other minor and major elements (Brady, 1995). Those measurements, together with a small ionic radius, suggest interstitial mechanism for Li diffusion in pyroxene and then a high-value for β (Schoen, 1958). The sole solid for which a value for β was found is silicon metal, for which β was found equal to its maximal value, ($\beta = 1/2$, Pell, 1960). In the case of silicate phases, the only estimate found, was measured for Li exchange between molten basalt and rhyolite ($\beta = 0.215$, Richter et al., 2003).

The value of β is however crucial in the modeling of the maximum isotopic fractionation produced between crystals (locally) and their surrounding groundmass. This maximum isotopic fractionation depends not only on β but also on the initial Li enrichment factor $[Li]_{crystal}/[Li]_{groundmass}$ (Fig. 7). Taking a Li enrichment factor of ≈0.23 (corresponding to the case observed in MIL 03346 where in the pyroxene core $[Li] = 2.3$ μg/g while in the rim $[Li] \approx 10$ μg/g) a minimum value for β of ≈0.15 is required to reproduce the range of δ^7Li values observed (≈20‰) (Fig. 7). We have chosen in the following to model the effect of diffusion for $\beta = 0.215$, as estimated by Richter et al. (2003) for silicate melts.

The temperature dependence of the diffusion coefficient (D_{Li}) can be expressed according to an Arrhenius law, $D_{Li} = D_0 \exp(-E_a/RT)$, where D_0 is the diffusion coefficient at infinite temperature, E_a is the activation energy and R is the ideal gas constant. In the case of pyroxene, $D_0 = 0.029$ m^2/s and $E_a = 258$ kJ (Coogan et al., 2005). Calculations were run using linear cooling rates from a starting temperature of $T_0 = 1000$ °C (solidus) to a final temperature of 600 °C.

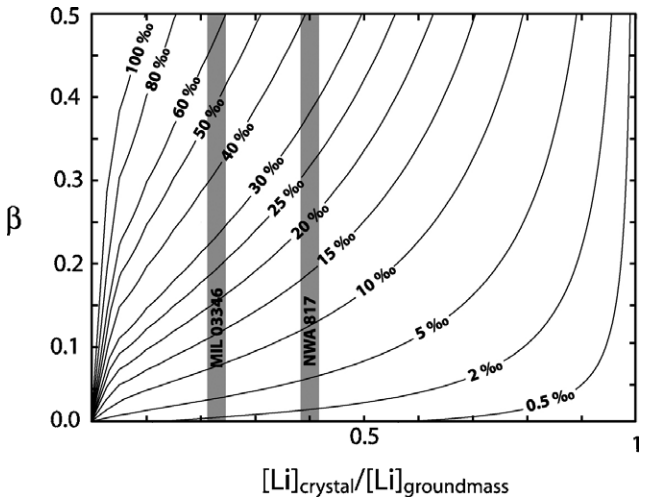

Fig. 7. Maximum isotopic variation in a 200 μm crystal as a function of the initial crystal to groundmass concentration ratio.

5.3. Implication of the diffusion model for phenocrysts from nakhlites

The [Li] and δ^7Li zoning profiles modeled for the relaxation of the [Li] gradients between the groundmass and the phenocrysts at various cooling rates are compared with the profiles observed for MIL 03346 and NWA 817 in Figs. 4 and 5. The enrichment factors used were of 0.23 ([Li] = 2.3 μg/g in the core of the crystal and [Li] = 10 μg/g in the rim, Table 2) for MIL 03346 and of 0.4 ([Li] = 4 μg/g is the lowest content found in pyroxene from this meteorite (Musselwhite et al., 2005) and [Li] = 10 μg/g in pyroxene rim, Table 2) for NWA 817.

The most important result from this modeling is that it demonstrates that the variety of Li distributions observed in the pyroxenes can be explained in a rather straightforward way from the redistribution of Li and of its isotopes by diffusion.

The calculations show that differential diffusion of the two lithium isotopes will create low δ^7Li edges (Figs. 4 and 5). For fast cooling rates, the isotopic composition of core of a 200 μm crystal is unaffected, but if the cooling rate is below about 50 K/h, the δ^7Li in the core will also decrease (Figs. 4 and 5). A very good fit is obtained between the modeled and the observed δ^7Li profiles and a fair fit with the Li concentration is observed. Cooling rates of 50 and 75 K/h are estimated for MIL 03346 and NWA 817, respectively. Our approach seems self consistent since the cooling rates, which give the best fit to the data, are similar for NWA 817 and MIL 03346, though the size of the two crystals studied differs.

Our implied cooling rates for NWA 817 and MIL 03346 are significantly higher than other estimates found in the literature. In the case of NWA 817 cooling rates calculated from Fe/Mg and Ca exchange at the interface between pyroxene and olivine are 0.5 and 2.2 K/h, respectively (Mikouchi and Miyamoto, 2002), while experimental petrography suggests a cooling rate of 3–6 K/h for MIL 03346 (Hammer and Rutherford, 2005). However, because the uncertainty on measured activation energy propagates along the cooling history, cooling rates calculations from diffusion are typically precise at one or two order of magnitude. As an example, cooling rates estimated for Nakhla using Ca or Fe/Mg diffusion result in almost a two orders of magnitude difference (Mikouchi and Miyamoto, 2002). In addition, we can remark that Li diffusivity for pyroxene was measured in Li enriched pyroxene (~2% atoms per formula unit) (Coogan et al., 2005). This high abundance may have fastened the diffusion process since favoring Li auto-diffusion. In the case of our studied crystals, Li concentrations are much lower (below 0.01% atoms per formula units) and auto-diffusion is prohibited.

In order to fit at best the δ^7Li profiles, δ^7Li values of +10‰ and of +17‰ had to be assumed for the groundmass of MIL 03346 and NWA 817, respectively. These values are higher than the terrestrial and/or chondritic δ^7Li values. Reported δ^7Li values range from $-3.8 + 0.6$‰ to $+3.9 \pm 0.6$‰ for bulk carbonaceous chondrites (James and Palmer, 2000; McDonough et al., 2003). δ^7Li values of fresh mid-oceanic ridge basalts are of ≈+3–4‰ (Chan et al., 1992; Moriguti and Nakamura, 1998; Nishio and Nakai, 2002), while the δ^7Li reported for bulk Martian meteorite lie between -0.6 ± 0.5‰ and $+5.2 \pm 0.5$‰ (Magna et al., 2006; Seitz et al., 2006).

Those heavy Li isotopic compositions are artificial since they are inherent to a limitation of our diffusion model. This model hypothesizes that the groundmass is an infinite reservoir, with thus a constant Li abundance and isotopic composition. However, through the diffusion history, as it looses Li, the groundmass will evolve toward heavier composition; the δ^7Li of the groundmass does not reflect the original magmatic isotopic composition. It can be pointed out that the δ^7Li values measured in NWA 817 pyroxene rims are higher that the measurements obtained in MIL 03346 pyroxene rims. This observation agrees well with the above proposition since Li abundances measured in pyroxenes are more equilibrated in NWA 817, than in MIL 03346.

Finally, Li concentrations increase from core to rim in Nakhla pyroxenes, though δ^7Li-values are rather constant (Fig. 3). If this concentration gradient was due to the addition of Li from the groundmass by diffusion, it should be associated to an isotopic fractionation. Because Nakhla contains a much smaller amount of groundmass than the two other meteorites studied (Nakhla (10 vol %) < NWA 817 (20 vol %) < MIL 03346 (22 vol %), Lentz et al., 1999; Sautter et al., 2002; Mikouchi et al., 2005), the magnitude of the effects due to Li diffusion in the phenocrysts might be different.

5.4. Is kinetic fractionation of Li by diffusion related to shock effects?

Diffusive effects on Li distribution seem thus widespread in meteorites from Mars. It is important to evaluate whether this process is specific to meteorites or to Martian meteorites or if it should be considered as a more general phenomenon occurring for terrestrial rocks. Because shock metamorphism is ubiquitous in Martian meteorites, the effects of such a shock must be evaluated to see whether they correspond or not to the temperature-time path required for Li diffusion to produce the effects observed in the present nakhlites.

Two shock effects can be expected. The first one is the "dynamic" escape of lithium, which is the direct consequence of crystal compression, and depends only on the peak shock pressure. Such a shock-induced devolatilization was produced for H and C during shock experiments on terrestrial and extra-terrestrial rocks (Tyburczy et al., 1990, 2001). However, the experiments performed by Chaklader et al. (2005) seem to indicate that this process does not apply to Li. The second effect is the diffusive relaxation of initial Li gradients during the temperature pulse associated with the shock event. This time-dependent pro-

cess cannot be realistically tested by shock experiments because of their too short duration but it can tentatively be quantified. During a shock, the compression of materials induces a simultaneous temperature and pressure increase according to the Hugoniot equations (Poirier, 1991). In the case of nakhlites, the peak temperature produced in the bulk rock is likely to be below 400 K only, as revealed by the calculation of augite Hugoniot (Malavergne et al., 2001). The peak temperature may even be lower according to Ar/Ar thermochronometry (Weiss and Shuster, 2005). Moreover, the shock duration is probably short, as revealed by the study of Zagami shock veins, for which the shock event lasted a few hundredth of second only (Beck et al., 2005). These low temperatures cannot produce any significant migration of Li during the shock events documented for Martian meteorites (for a temperature pulse of 400 K lasting 20×10^{-3} s, the diffusion length of Li in albite is below an Angstrom). Alternatively, temperatures above 2400 K can be produced locally by frictional heating (Chen et al., 1996), within shear-melt-veins (SMVs) or melt pockets (MP). Close to these "hot spots" a substantial migration of Li would be possible (during 20×10^{-3} s at 2400 K, the diffusion length of Li in albite is 40 μm). However SMVs and MPs have never been observed yet in nakhlites. In the case of NWA 480, melt pockets are present in the meteorite, but they lack in the surroundings of the studied pyroxene. Thus, it seems reasonable to think that the Li distributions of nakhlites and shergottites were only moderately affected during their ejection from Mars.

If shocks are not the source of the diffusion processes, then Li elemental and isotopic redistributions can be expected to occur during the post-magmatic evolution of terrestrial porphyritic rocks having a cooling history equivalent to that of nakhlites (1–100 K/h). It seems necessary to perform similar studies on terrestrial samples, in order to investigate the local effects of diffusion in crystal, and the length scale of Li isotopic heterogeneities in bulk samples.

6. Conclusions

In NWA 817 and MIL 03346 nakhlites, large Li isotopic variations, decoupled from the variations of Li abundances, were found within augite crystals. Martian or terrestrial weathering, involvement of a high-δ^7Li reservoir, shock metamorphism, or degassing processes can account neither for the ranges of δ^7Li values, nor the shapes of the profiles in Li concentrations and isotopic compositions. A viable mechanism to produce these complex Li distributions seems to be post-magmatic diffusive exchange of Li between crystals and groundmass. Though the feasibility of such a process can be established by modeling, it is obvious that experimental data are lacking for the diffusivities of the two isotopes in pyroxene and olivine.

Since the initial Li magmatic record was perturbed by diffusion processes in two of the three studied nakhlites, the use of Li as an indicator of degassing processes appears questionable. Our calculations suggest that even a very restricted amount of diffusion can produce large isotopic variations (>20‰). In Nakhla, the isotopic variation we measured is more restricted, and the initial Li zoning could be preserved. This difference could be explained by a smaller amount of groundmass in Nakhla that in the other samples studied or from geometric effects. In other crystals from the same section or in another section, large δ^7Li variations may be measured.

Acknowledgments

The Nakhla and MIL 03346 sections were kindly provided by the Muséum National d'Histoire Naturelle de Paris and by the Meteorite Working Group. This project would probably not be achieved without the kind help of Denis Mangin, Michel Champenois and Claire Rollion-Bard during the SIMS sessions. We thank R.L. Hervig for the editorial handling, D.J. Cherniak, A.H. Treiman and an anonymous reviewer for constructive comments. We gratefully acknowledge the Programme National de Planétologie (INSU) for financial support. This research has made use of NASA's Astrophysics Data System Abstract Service and the now indispensable Martian meteorites compendium written by Chuck Meyer.

Associate editor: Richard L. Hervig

References

Barrat, J.A., Chaussidon, M., Bohn, M., Gillet, P., Göpel, C., Lesourd, M., 2005. Lithium behavior during cooling of a dry basalt: an ion-microprobe study of the lunar meteorite Northwest Africa 479 (NWA 479). *Geochim. Cosmochim. Acta* **69**, 5597–5609.

Barrat, J.A., Benoit, M., Cotten, J., 2006. Bulk chemistry of the nakhlite Miller Range 03346 (MIL 03346). *Lunar Planet. Sci. Conf.* **37**, #1569 abstract.

Beck, P., Barrat, J.A., Chaussidon, M., Gillet, Ph., Bohn, M., 2004. Li isotopic variations in single pyroxene from the Northwest Africa 480 (NWA 480) shergottite: a record of degassing of martian magmas? *Geochim. Cosmochim. Acta* **68**, 2925–2933.

Beck, P., Gillet, P., El Goresy, A., Mostefaoui, I., 2005. Timescales of shock processes in chondritic and Martian meteorites. *Nature* **435**, 1071–1074.

Brady, J.B., 1995. Diffusion data for silicate minerals, glasses and liquids. In: Ahrens, T.J. (Ed.), *A Handbook of Physical Constants, Mineral Physics and Crystallography*, vol. 2. American Geophysical Union.

Brenan, J.M., Neroda, E., Lundstrom, C.C., Shaw, H.F., Ryerson, F.J., Phinney, D.L., 1998a. Behaviour of boron, beryllium, and lithium during melting and crystallization: constraints from mineral-melt partitioning experiments. *Geochim. Cosmochim. Acta* **62**, 2129–2141.

Brenan, J.M., Ryerson, F.J., Shaw, H.F., 1998b. The role of aqueous fluids in the slab-to-mantle transfer of boron, beryllium, and lithium during subduction: experiments and models. *Geochim. Cosmochim. Acta* **62**, 3337–3347.

Bridges, J.C., Grady, M.M., 2000. Evaporite mineral assemblages in the nakhlite (martian) meteorites. *Earth Planet. Sci. Lett.* **176**, 267–279.

Bridges, J.C., James, R.H., Pearson, V.K., Baker, L., Verchovsky, A.B., Wright, I.P., 2005. Lithium and carbon isotopic fractionation between

the alteration assemblages of Nakhla and Lafayette. *Lunar Planet. Sci. Conf.* **36**, #1758 abstract.

Chaklader, J., Shearer, C.K., Hörz, F., 2005. Li, B—behavior in lunar basalts during shock and thermal metamorphism: implications for H_2O in Martian magmas. *Lunar and Planet. Sci. Conf.* **36**, #1426 abstract.

Chan, L.H., Edmond, J.M., Thompson, G., Gillis, K., 1992. Lithium isotopic composition of submarine basalts-implications for the lithium cycle in the oceans. *Earth Planet. Sci. Lett.* **108**, 151–160.

Chan, L.H., Edmond, J.M., Thompson, G., 1993. A lithium isotope study of hot-springs and metabasalts from mid-ocean ridge hydrothermal systems. *J. Geophys. Res.* **98**, 9653–9659.

Chaussidon, M., Robert, F., 1998. $^{7}Li/^{6}Li$ and $^{11}B/^{10}B$ variations in chondrules from the Semarkona unequilibrated chondrite. *Earth Planet. Sci. Lett.* **164**, 577–589.

Chen, M., Sharp, T.G., El Goresy, A., Wopenka, B., Xie, X., 1996. The majorite-pyrope-magnesiowüstite assemblage: constraints on the history of shock veins in chondrite. *Science* **271**, 1570–1573.

Coogan, L.A., Kasemann, S.A., Chakraborty, S., 2005. Rates of hydrothermal cooling of new upper oceanic crust derived from lithium-geospeedometry. *Earth Planet. Sci. Lett.* **240**, 415–424.

Crank, J., 1967. *The Mathematics of Diffusion*. Oxford University Press, London, 414 pp.

Dann, J.C., Holzheid, A.H., Grove, T.L., McSween Jr., H.Y., 2001. Phase equilibria of the Shergotty meteorite: Constraints on pre-eruptive water contents of Martian magmas and fractional crystallization under hydrous conditions. *Meteorit. Planet. Sci.* **36**, 793–806.

Decitre, S., Deloule, E., Reisberg, L., James, R., Agrinier, P., Mevel, C., 2002. Behavior of Li and its isotopes during serpentinization of oceanic peridotites. *Geochem. Geophys. Geosyst.* **3**.

DePaolo, D.J., 1981. Trace element and isotopic effects of combined wallrock assimilation and fractional crystallization. *Earth Planet. Sci. Lett.* **53**, 189–202.

Dreibus, G., Palme, H., Rammensee, W., Spettel, B., Weckwerth, G., Wanke, H., 1982. Composition of Shergotty parent body: further evidence for a two component model of planet formation. *Lunar Planet. Sci. Conf.* **13**, #186-17 abstract.

Elliott, T., Jeffcoate, A., Bouman, C., 2004. The terrestrial Li isotope cycle: light-weight constraints on mantle convection. *Earth Planet. Sci. Lett.* **220**, 231–245.

Flesh, G.D., Anderson, A.R., Svec, H.J., 1973. A secondary isotopic standard for $^{7}Li/^{6}Li$ determination. *Int. J. Mass Spectrom. Ion Phys.* **12**, 265–272.

Giletti, B.J., Shanahan, T.M., 1997. Alkali diffusion in plagioclase feldspar. *Chem.l Geol.* **139**, 3–20.

Gillet, Ph., Barrat, J.A., Deloule, E., Wadhwa, M., Jambon, A., Sautter, V., Devouard, B., Neuville, D., Benzerara, K., Lesourd, M., 2002. Aqueous alteration in the Northwest Africa 817 (NWA 817) Martian meteorite. *Earth Planet. Sci. Lett.* **203**, 431–444.

Hammer, J.E., Rutherford, M.J., 2005. Experimental crystallization of Fe-rich basalt: application to cooling rate and oxygen fugacity of nakhlite MIL-03346. *Lunar Planet. Sci. Conf.* **36**, #1999 abstract.

Herd, C.D.K., Treiman, A.H., McKay, G.A., Shearer, C.K., 2002. Experimental lithium and boron partition coefficients: implications for magmatic water in Martian meteorites. *Lunar Planet. Sci. Conf.* **33**, #1333 abstract.

Herd, C.D.K., Treiman, A.H., McKay, G.A., Shearer, C.K., 2004. The behavior of Li and B during planetary basalt crystallization. *Am. Mineralogist* **89**, 832–840.

Herd, C.D.K., Treiman, A.H., McKay, G.A., Shearer, C.K., 2005. Light lithophile elements in martian basalts: evaluating the evidence for magmatic water degassing. *Geochim. Cosmochim. Acta* **69**, 2431–2440.

Jambon, A., 1980. Isotopic fractionation—a kinetic-model for crystals growing from magmatic melts. *Geochim. Cosmochim. Acta* **44**, 1373–1380.

James, R.H., Palmer, M.R., 2000. The lithium isotope composition of international rock standards. *Chem. Geol.* **166**, 319–326.

Lentz, R.C.F., Taylor, G.J., Treiman, A.H., 1999. Formation of a martian pyroxenite: a comparative study of the nakhlite meteorites and Theo's Flow. *Meteorit. Planet. Sci.* **34**, 919–932.

Lentz, R.C.F., McSween, H.Y., Ryan, J., Riciputi, L.R., 2001. Water in martian magmas: clues from light lithophile elements in shergottite and nakhlite pyroxenes. *Geochim. Cosmochim. Acta* **65**, 4551–4565.

Lundstrom, C.C., Chaussidon, M., Hsui, A.T., Kelemen, P., Zimmerman, M., 2005. Observations of Li isotopic variations in the Trinity ophiolite: evidence for isotopic fractionation by diffusion during mantle melting. *Geochim. Cosmochim. Acta* **69**, 735–751.

Magna, T., Wiechert, U., Halliday, A.N., 2006. New constraints on the lithium isotope composition of the Moon and terrestrial planets. *Earth Planet. Sci. Lett.* **243**, 336–353.

Malavergne, V., Guyot, F., Benzerara, K., Martinez, I., 2001. Description of new shock-induced phases in the Shergotty, Zagami, Nakhla and Chassigny meteorites. *Meteorit. Planet. Sci.* **36**, 1297–1305.

McDonough, W.F., Teng, F.Z., Tomascak, P.B., Ash, R.D., Grossman, J.N., Rudnick, R.L., 2003. Lithium isotopic composition of chondritic meteorites (abstract). *Lunar Planet. Sci.* **34**, #1931.

Mikouchi, T., Miyamoto, M., 2002. Comparative cooling rates of nakhlites as inferred from iron-magnesium and calcium zoning of olivines. *Lunar Planet. Sci. Conf.* **33**, #1343 abstract.

Mikouchi, T., Monkawa, A., Koizumi, E., Chokai, J., Miyamoto, M., 2005. MIL03346 Nakhlite and NWA2737 "Diderot" Chassignite: two new Martian cumulate rocks from hot and cold deserts. *Lunar Planet. Sci. Conf.* **36**, #1944 abstract.

Moriguti, T., Nakamura, E., 1998. High-yield lithium separation and the precise isotopic analysis for natural rock and aqueous samples. *Chem. Geol.* **145**, 91–104.

Musselwhite, D.S., Treiman, A.H., Shearer, C.K., 2005. Light lithophile element trends in nakhlite NWA 817 pyroxenes: implications for water on Mars. *Lunar Planet. Sci. Conf.* **36**, #1230 abstract.

Nishio, Y., Nakai, S., 2002. Accurate and precise lithium isotopic determinations of igneous rock samples using multi-collector inductively coupled plasma mass spectrometry. *Analyt. Chim. Acta* **456**, 271–281.

Pell, E.M., 1960. Diffusion of Li in Si at high-T and the isotope effect. *Phys. Rev.* **119**, 1014–1021.

Peterson, N.L., Chen, W.K., 1974. Correlation and isotope effects for cation diffusion in simple oxides. In: Cooper, A.R., Heuer, A.H. (Eds.), *Mass Transport Phenomena in Ceramics*, *Materials Science Research*, vol. 9. Plenum press, New York.

Poirier, J.P., 1991. *Introduction to the Physics of the Earth's interior*. Cambridge University Press, Cambridge, 312 pp.

Richter, F.M., Liang, Y., Davis, A.M., 1999. Isotope fractionation by diffusion in molten oxides. *Geochim. Cosmochim. Acta* **63**, 2853–2861.

Richter, F.M., Davis, A.M., DePaolo, D.J., Watson, E.B., 2003. Isotope fractionation by chemical diffusion between molten basalt and rhyolite. *Geochim. Cosmochim. Acta* **67**, 3905–3923.

Sautter, V., Barrat, J.A., Jambon, A., Lorand, J.P., Gillet, Ph., Javoy, M., Joron, J.L., Lesourd, M., 2002. A new Martian meteorite from Morocco: the nakhlite North West Africa 817. *Earth Planet. Sci. Lett.* **195**, 223–238.

Schoen, A.H., 1958. Correlation and the isotope effect for diffusion in crystalline solids. *Phys. Rev. Lett.* **1**, 138–140.

Seitz, H.S., Brey, G.P., Weyer, S., Durali, S., Ott, U., Münker, C., Mezger, K., 2006. Lithium isotope composition of Martian and Lunar reservoirs. *Earth Planet. Sci. Lett.* **245**, 6–18.

Teng, F.Z., McDonough, W.F., Rudnick, R.L., Walker, R.J., 2006. Diffusion-driven extreme lithium isotopic fractionation in country rocks of the Tin Mountain pegmatite. *Earth Planet. Sci. Lett.* **243**, 701–710.

Tomascak, P.B., 2004. Developments in the understanding and application of lithium isotopes in the Earth and planetary Sciences. In: Johnson, C.M., Beard, B.L., Albarède, F. (Eds.), *Geochemistry of Non-Traditional Stable Isotopes*, vol. 55. The Mineralogical Society of America.

Tomascak, P.B., Tera, F., Helz, R.T., Walker, R.J., 1999. The absence of lithium isotope fractionation during basalt differentiation: new measurements by multicollector sector ICP-MS. *Geochim. Cosmochim. Acta* **63**, 907–910.

Treiman, A.H., 2005. The nakhlite meteorites: augite-rich igneous rocks from Mars. *Chemie. Erde-Geochem.* **65**, 203–270.

Tyburczy, J.A., Krishnamurthy, R.V., Epstein, S., Ahrens, T.J., 1990. Impact-induced devolatilization and hydrogen isotopic fractionation of serpentine: implications for planetary accretion. *Earth Planet. Sci. Lett.* **98** (2), 245.

Tyburczy, J.A., Xu, X., Ahrens, T.J., Epstein, S., 2001. Shock-induced devolatilization and isotopic fractionation of H and C from Murchison meteorite: some implications for planetary accretion. *Earth Planet. Sci. Lett.* **192** (1), 23.

Weiss, B.P., Shuster, D.L., 2005. Martian surface paleotemperatures from thermochronometry of meteorites. *Lunar Planet. Sci. Conf.* **36**, #1156 abstract.

You, C.F., Chan, L.H., Spivack, A.J., Gieskes, J.M., 1995. Lithium, boron, and their isotopes in sediments and pore waters of Ocean Drilling Program site 808, Nankai trough: implications for fluid expulsion in accretionary prisms. *Geology* **23**, 37–40.

Zack, T., Tomascak, P.B., Rudnick, R.L., Dalpé, C., McDonough, W.F., 2003. Extremely light Li in orogenic eclogites: the role of isotope fractionation during dehydration in subducted oceanic crust. *Earth Planet. Sci. Lett.* **208**, 279–290.

Zanetti, A., Tiepolo, M., Oberti, R., Vannucci, R., 2004. Trace-element partitioning in olivine: modelling of a complete data set from a synthetic hydrous basanite melt. *Lithos* **75**, 39–54.